

# Growth and characterisation of GaAs/InGaAs/GaAs nanowhiskers on (1 1 1) GaAs

I. Regolin<sup>a,\*</sup>, D. Sudfeld<sup>b</sup>, S. Lüttjohann<sup>c</sup>, V. Khorenko<sup>a</sup>, W. Prost<sup>a</sup>, J. Kästner<sup>b</sup>,  
G. Dumpich<sup>b</sup>, C. Meier<sup>c</sup>, A. Lorke<sup>c</sup>, F.-J. Tegude<sup>a</sup>

<sup>a</sup>*Solid State Electronics Department, University of Duisburg-Essen, Lotharstr. 55, ZHO, D-47048 Duisburg, Germany*

<sup>b</sup>*Department of physics, Experimental Physics, AG Farle, University of Duisburg-Essen, Lotharstr. 1, D-47048, Duisburg, Germany*

<sup>c</sup>*Laboratorium für Festkörperphysik, University of Duisburg-Essen, Lotharstr. 1, D-47048 Duisburg, Germany*

Available online 28 November 2006

## Abstract

GaAs/In<sub>x</sub>Ga<sub>1-x</sub>As/GaAs heterostructures nanowires were grown by metal-organic vapor-phase epitaxy on (1 1 1)B GaAs substrate using the vapor–liquid–solid growth mode. The diameter of the nanowires was defined by monodisperse gold nanoparticles deposited on the GaAs substrate. High-resolution electron transmission microscopy investigation revealed the structural properties of the grown whiskers using bright field images. Using energy disperse X-ray spectroscopy measurements, the composition along and perpendicular to the vertical growth direction has been determined. In addition, the sharpness of the created heterojunctions was investigated. Finally, micro photoluminescence measurements on single GaAs/InGaAs/GaAs whiskers were carried out.

© 2006 Elsevier B.V. All rights reserved.

**Keywords:** A1. High-resolution electron transmission microscopy; A1. Nanostructures; A3. Metalorganic vapor phase epitaxy; B1. Arsenates; B1. Gallium compounds; B2. Semiconducting III–V materials

## 1. Introduction

Semiconductor nanowhiskers excite a great research interest due to their intriguing growth features as well as a potential application in nanoscale electronic and optoelectronic devices. Based on the vapour–liquid–solid (VLS) growth mechanism [1] using Au seed particles or templates various semiconductor nanowhiskers have been reported. Shrinking the Au seed to the nanometer scale and using the metal-organic vapor phase epitaxy technique [2] enabled the realization of highly mismatched one-dimensional semiconductor heterostructures [3,4]. Despite a good progress in the growth of elementary and binary materials, there is a lack of studies on ternary compounds and their heterointerfaces. The change of group-III elements was only published once in 1994 by forming a heterojunction between GaAs and InAs along the vertical growth direction [5]. These structures are indispensable for band

gap engineered devices i.e. for III/V-based optoelectronics at 1.3/1.55 μm on a Si substrate [6,7]. However, the VLS growth takes place at low temperatures, which may result in a non-linear dependence of the precursor cracking and different incorporation efficiency in the whisker. In addition, the range of growth temperature variation is further limited by potential whisker kinking [8] and parasitic 2-dimensional growth.

In this contribution, we report the growth of high-quality GaAs/In<sub>x</sub>Ga<sub>1-x</sub>As/GaAs heterostructures on (1 1 1)B GaAs substrate. We have developed a growth temperature sequence, which enables both the incorporation of a full set of In-compositions as well as wire-kinking-free heterointerfaces. This approach became feasible by means of two different gallium precursors with different incorporation efficiencies adapted to the required growth condition. The structure and the lattice parameter of the grown structures were determined by high-resolution transmission microscopy (HR-TEM) measurements using bright-field images. The composition at the different whisker regions was analyzed using energy disperse X-ray

\*Corresponding author. Tel.: +49 203 379 3877; fax: +49 203 379 3400.  
E-mail address: [regolin@hlt.uni-duisburg.de](mailto:regolin@hlt.uni-duisburg.de) (I. Regolin).

spectroscopy (EDS) as well as micro-photoluminescence ( $\mu$ -PL).

## 2. Experimental procedure

Growth experiments were performed in a low-pressure MOVPE using an AIX200 RF low-pressure system with a full non-gaseous source configuration [9].  $N_2$  was used as carrier gas and tertiarybutylarsine (TBAs) as group-V precursor. Trimethylindium (TMIn) was used as In precursor while both trimethylgallium (TMGa) and triethylgallium (TEGa) were used as Ga precursors. As a growth seed Au nanoparticles in a colloidal solution deposited on the substrate surface prior to the growth were used. The mean diameter of the used particles was 102.3 nm with a variation  $<8\%$  for the GaAs/InGaAs/GaAs structures, resulting in a surface density of about  $10^8 \text{ cm}^{-3}$ . InGaAs structures for the X-ray characterisation were grown, using particles with a mean diameter of 9.8 nm and a variation  $<10\%$ , with densities of about  $10^9 \text{ cm}^{-3}$ . Detailed analyses about the nanowhisker formation depending on the particle size and surface density are reported elsewhere [10,11].

After annealing the GaAs substrates at  $600^\circ\text{C}$  for 10 min under TBAs flow, the temperature was ramped down to the growth temperature. The whisker growth was carried out at a total pressure of 50 mbar and a total gas flow of 3.41/min, respectively, whereas the V/III ratio was varied between 5 and 10. A total growth time around 10 min was chosen to realize structures up to  $5 \mu\text{m}$  in length to simplify the following analyses.

The as-grown nanowhiskers were inspected by SEM using a LEO 1530 microscope. The composition of homogeneous whiskers was characterized by high-resolution X-ray diffraction using a STOE STADIP triple-crystal diffractometer using  $\text{Cu K}\alpha_1$  radiation and a scintillation counter as a detector. The diffraction curves are recorded in the vicinity of the symmetric (111) reflections. For further characterization the whiskers were scratched from the substrate surface and solved in isopropanol. The whisker suspension was then dropped onto a suitable substrate. For TEM characterization including EDS analysis the whiskers were dropped onto a commercial TEM grid. The measurements were done using a Philips Tecnai F20ST microscope.  $\mu$ -PL measurements with excitation intensity of 0.36 mW and spot diameter of about  $1 \mu\text{m}$  were performed at 4.2 K on single whiskers, which were transferred to a Si wafer.

## 3. Results

In a first step  $\text{In}_x\text{Ga}_{1-x}\text{As}$  nanowhiskers with various homogenous In-compositions  $x$  were grown. The TMIn/(TMIn + TEGa) ratio was varied from 0.038 to 0.452. The TMIn supply was changed resulting in the significant increase of a total TMIn + TEGa gas flow and consequently in a higher growth rate for In-rich structures.

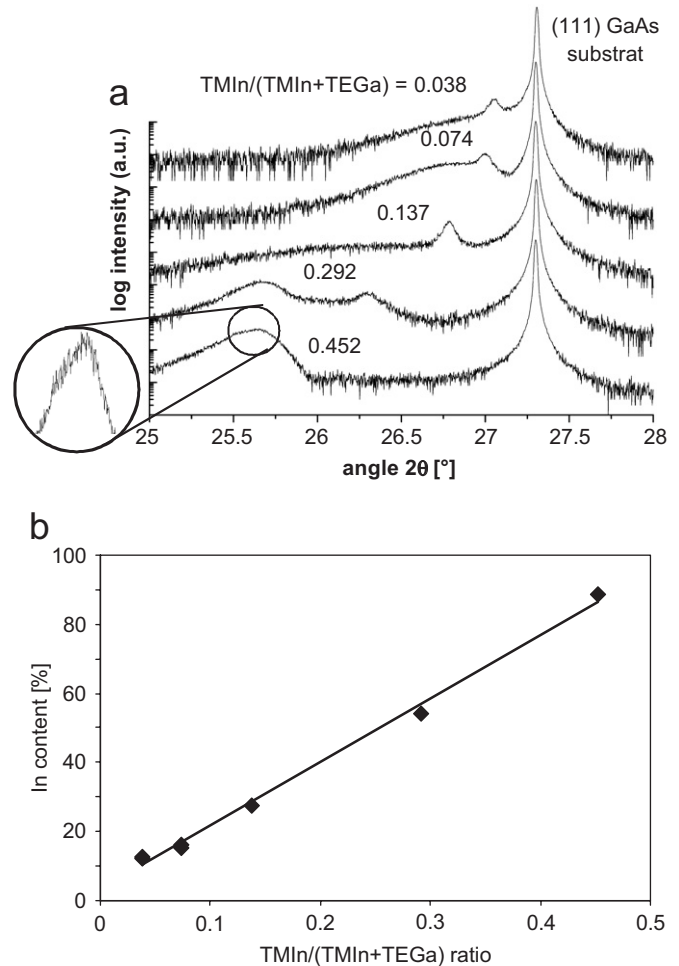


Fig. 1. (a) XRD rocking curves of InGaAs nanowhisker structures grown using various TMIn/(TMIn + TEGa) ratios. (b) In content as a function of TMIn mole fraction, extracted from XRD measurements.

Fig. 1a shows XRD rocking curves of fabricated structures. The whisker peaks and the 2-dimensional  $\text{In}_x\text{Ga}_{1-x}\text{As}$  layer peaks can be clearly resolved. Depending on the chosen TMIn/(TMIn + TEGa) ratio, the peaks shift between the GaAs peak at  $27.301^\circ$  and the InAs peak at  $25.444^\circ$ . From the position of the whisker peak, a corresponding indium concentration of 14%, 16.4%, 27.6%, 54.3% and 88.6% was calculated (Fig. 1b). The In content of the whisker structures was calculated using a linear correlation to the peak positions. This simplified analyses neglects the Poisson ratio, because a full-relaxation of the whisker lattice is assumed. The calculated compositions were verified by TEM measurements using bright-field images and evaluated according to [5]. The results demonstrate that the full regime of In-compositions is available.

Next, the growth of GaAs/ $\text{In}_x\text{Ga}_{1-x}\text{As}$ /GaAs nanowhisker heterostructures is discussed. The GaAs parts were grown using TMGa. The growth temperature of the lower GaAs part was fixed at  $480^\circ\text{C}$  while the growth temperature of the upper part was varied between  $480$  and  $530^\circ\text{C}$ .

The InGaAs parts were grown at 420 °C using TEGa and TMIIn. An In-content of approximately  $x = 0.5$  was adjusted.

In the following the results of a GaAs/In<sub>x</sub>Ga<sub>1-x</sub>As/GaAs nanowhisker heterostructure are presented where the growth temperature of the upper GaAs part was set to 480 °C. The bright field TEM image in Fig. 2a indicates that despite the low growth temperature for the upper part a tapering effect can be observed. This specific shape led to the whisker model, which is given in Fig. 2b. It assumes an additional GaAs shell over the whole structure as well as an additional InGaAs inner shell at the bottom part. Because of this configuration EDS line scans perpendicular to the vertical growth directions in the three characteristic regions were done and shown in Fig. 3. While the top part shows only GaAs as expected (a), the middle InGaAs part shows an additional GaAs shell with around 30 nm in thickness (b). The In content of the core could be calculated by subtraction of the GaAs shell up to around 50%. The GaAs bottom part in (c) shows even two additive shells. The outer 30 nm GaAs shell is the same as in the middle region. In addition, the InGaAs growth of the middle region resulted in an inner InGaAs shell with a thickness of around 80 nm around the bottom GaAs part of the heterostructure whisker. The In content of both the shell and the InGaAs part is around  $x = 0.5$ . The chosen growth temperatures cause additional 2-dimensional growth, which is stronger for the InGaAs part.

The overlay of lateral and vertical heterojunction in the whisker complicates the determination of the composition across the heterojunctions. Following the schematic model in Fig. 2b, the identification of from the InGaAs middle part to the top GaAs part should best suited. Only the influence of the GaAs shell has to be taken into account. The measured line scan in this region is given in Fig. 4. The existence of a sharp heterojunction could not be observed. In contrast, the In content changes over a few hundred

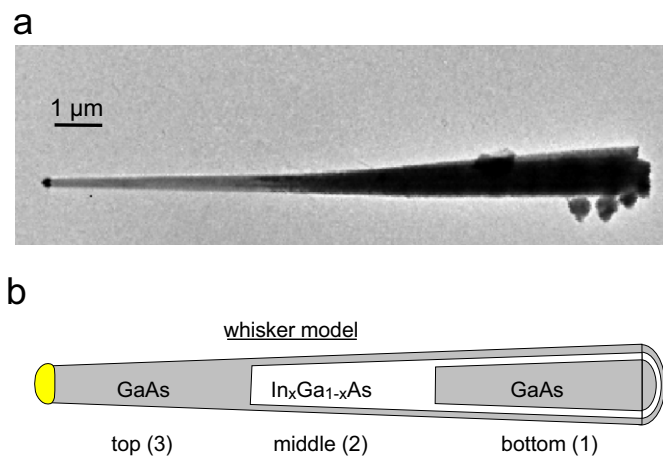


Fig. 2. TEM bright field image of GaAs/InGaAs/GaAs whiskers grown on GaAs (111) substrate using 480 °C for the upper GaAs part (a). Whisker model including a core-shell structure in the middle part, as well as a double-shelled structure at the bottom (b).

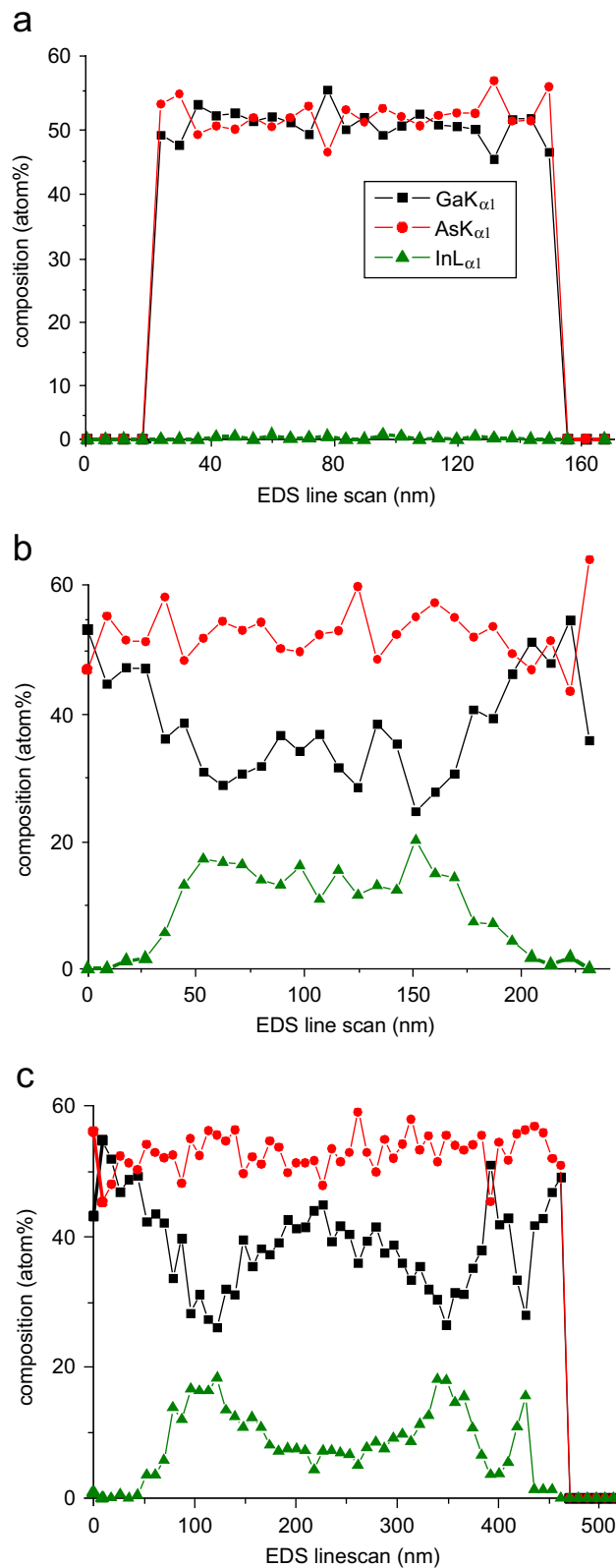


Fig. 3. EDS line scans perpendicular to the growth direction in the tree characteristic regions. GaAs at the upper part (a), InGaAs core shelled with 30 nm GaAs at the middle part (b) and the double-shell structure at the bottom (c).

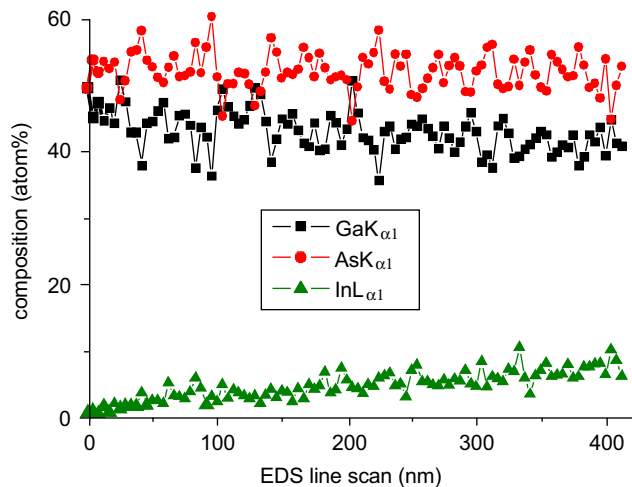


Fig. 4. EDS line scan in vertical growth direction from the GaAs top part to the InGaAs middle part.

nanometers. We suppose that this effect is driven by the memory effect of the group-III elements in the Au droplet, which prevents the creation of sharp heterointerfaces.

To enforce the creation of core-shell structures, nano-whiskers using a higher temperature for the upper GaAs part were grown. Fig. 5a shows a SEM micrograph of GaAs/InGaAs/GaAs whiskers, where the upper part was grown at 510 °C. Besides the stronger tapering effect, a wire-kinking at all structures is visible. This kinking is attributed to instability at the InGaAs/GaAs interface during the temperature rise-up. To overcome the wire kinking for the creation of core-shell structures, we have developed a multiple step temperature sequence for the growth temperature after InGaAs growth. At first, the temperature is increased up to 480 °C and then GaAs is grown for 3 min. This step prevents the formation of kinking at the InGaAs/GaAs interface. Next, without any growth stop, the growth temperature increases to 530 °C during 2.5 min. Finally, the growth was carried-out at 530 °C for 9.5 min in order to create a thick GaAs shell. In Fig. 5b a SEM micrograph of the resulting kink-free GaAs/InGaAs/GaAs core-shell whiskers is shown.

The GaAs/InGaAs/GaAs core-shell whiskers with a thick shell are analyzed with EDS. Fig. 6 presents an EDS line scan across the middle InGaAs part of the whisker including an around 200 nm thick outer GaAs shell. Because of this thick shell, the In content seems very low in the quantified line scan. The subtraction of the GaAs shell gives an In content around 50% as calculated for the thinner structures.

To investigate the optical properties of the grown structures,  $\mu$ -PL measurements in the GaAs-related wavelength regime from 810 to 890 nm on single whisker structures like in Fig. 2a were made. A high intensity of the PL signal confirms a good crystalline quality. Fig. 7 shows the spectra taken at different positions along a single whisker. Besides the GaAs band gap peak at 820 nm, some impurity peaks are observed at higher wavelengths around

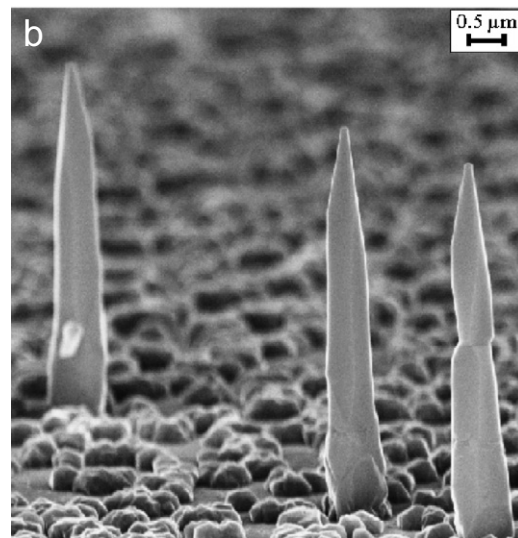
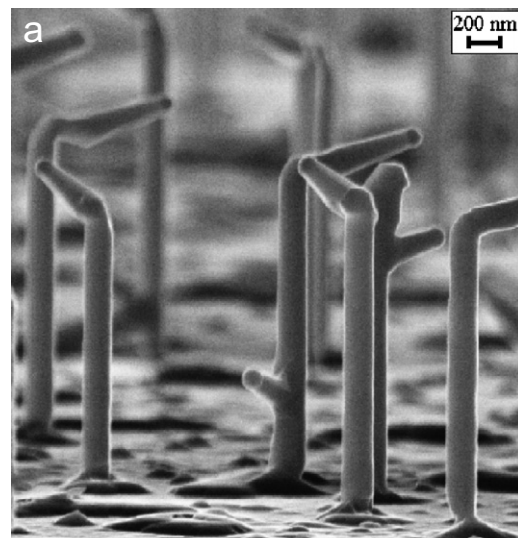


Fig. 5. SEM micrograph of kinked whiskers at the InGaAs/GaAs interface as result of unbalance at the growth front during the temperature ramp to 510 °C (a) and non-kinked structures with a thick additional grown GaAs shell (c).

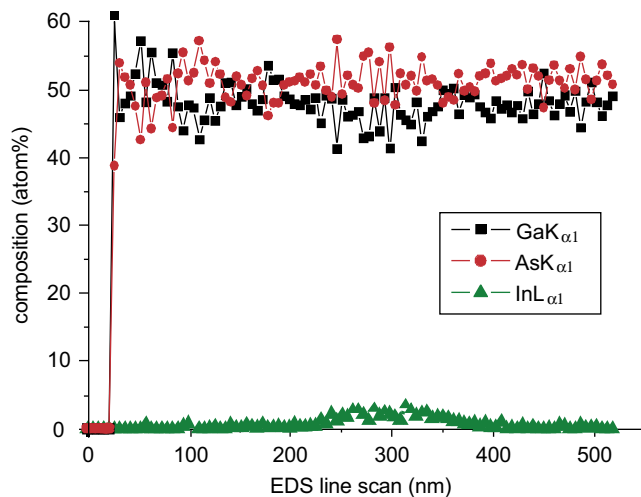


Fig. 6. EDS line scans perpendicular to the growth direction at the InGaAs middle part shows an additive GaAs shell of around 150 nm thickness.

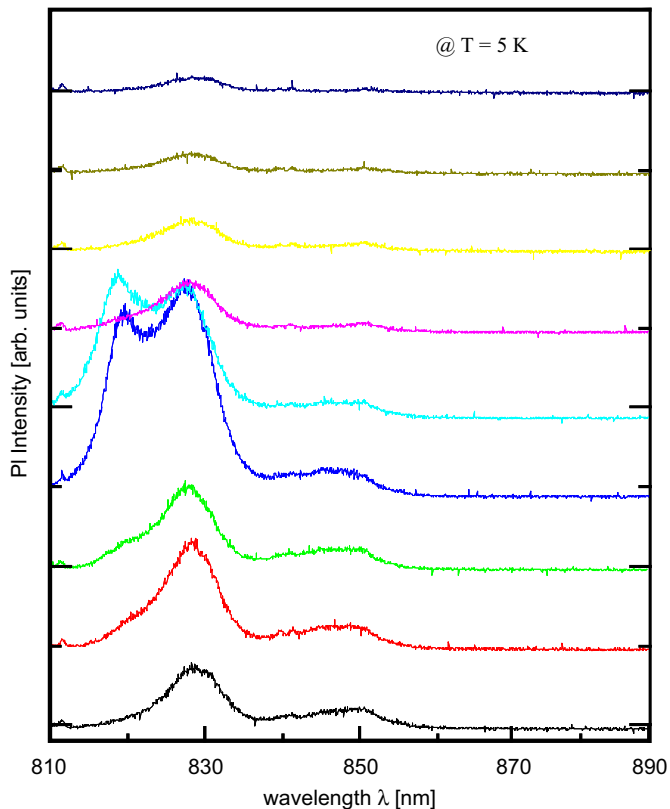


Fig. 7.  $\mu$ -PL measurements taken at various points along the whisker length representing the GaAs part and some impurity peaks (b).

830 and 850 nm. Peaks due to the InGaAs with an In content up to around 50% could not be detected, because in the limitation of the CCD detector with a maximum of 1050 nm in wavelength. No PL-signal was detected outside the whisker confirming that the whisker is the physical origin of the PL.

#### 4. Conclusion

GaAs/In<sub>x</sub>Ga<sub>1-x</sub>As/GaAs heterostructures nanowhisker grown in the VLS mode exhibit in a wide temperature range both lateral and vertical heterojunctions, respectively. The properties of the vertical junction in the direction of whisker growth are defined by the VLS growth mode. By means of EDS line scans no sharp InGaAs/GaAs heterojunctions were found in the vertical direction attributed to a memory effect of the group-III species in

the Au droplet. The lateral heterojunctions of the core-shell structure are defined by an additional 2-dimensional growth comparable to conventional epitaxial layer growth. In the vertical growth direction EDS line scans indicate a sharp core-shell GaAs/InGaAs/GaAs heterojunction. The photoluminescence of GaAs-related emissions showed a high PL intensity of single GaAs/In<sub>x</sub>Ga<sub>1-x</sub>As/GaAs whiskers. Depending on the adjusted growth temperature for the upper GaAs part the thickness of the shell can be adjusted. The upper InGaAs/GaAs heterojunction requires a temperature rise, which may result in wire kinking. Wire-kinking-free heterointerfaces have been grown using (i) a multiple temperature grading at the junction and (ii) using two different gallium precursors with different incorporation efficiencies adapted to the required growth condition.

#### Acknowledgments

The authors acknowledge financial support of the Sonderforschungsbereich SFB 445.

#### References

- [1] R.S. Wagner, W.C. Ellis, *Appl. Phys. Lett.* 4 (1964) 89.
- [2] K. Hiruma, T. Katsuyama, K. Ogawa, M. Koguchi, G.P. Morgan, H. Kakibayashi, *Appl. Phys. Lett.* 59 (1991) 431.
- [3] M. Bjoerk, B.J. Ohlsson, T. Sass, A.I. Persson, C. Thelander, M.H. Magnusson, K. Deppert, L.R. Wallenberg, L. Samuelson, *Nano Lett.* 2 (2002) 87.
- [4] V. Khorenko, I. Regolin, S. Neumann, H. Wiggers, W. Prost, F.-J. Tegude, *Appl. Phys. Lett.* 85 (2004) 6407.
- [5] K. Hiruma, H. Murakoshi, M. Yazawa, K. Ogawa, S. Fukuhara, M. Shirai, T. Katsuyama, *IEICE Trans. Electron. E 77-C (9)* (1994).
- [6] T. Martensson, C. Svensson, B. Wacaser, M. Larsson, W. Seifert, K. Deppert, A. Gustavsson, L. Wallenberg, L. Samuelson, *Nano Lett.* 4 (2004) 10.
- [7] I. Regolin, V. Khorenko, W. Prost, F.-J. Tegude, *J. Appl. Phys.* 2005, accepted for publication.
- [8] J. Westwater, D.P. Gosain, S. Tomiya, S. Usui, H. Ruda, *J. Vac. Sci. Technol. B* 15 (3) (1997) 554.
- [9] P. Velling, *Progress in Crystal Growth and Characterisation of Materials*, vol. 41, 2000, p. 85.
- [10] W. Seifert, M. Borgström, K. Deppert, K.A. Dick, J. Johansson, M.W. Larsson, T. Martensson, N. Sköld, C.P. Svensson, B.A. Wacaser, L.R. Wallenberg, L. Samuelson, *J. Crystal Growth* 272 (2004) 211.
- [11] L.E. Jensen, M.T. Björk, S. Jeppesen, A.I. Persson, B.J. Ohlsson, L. Samuelson, *Nano Lett.* 4 (2004) 10.